Interhemispheric asymmetry of the high-latitude ionospheric convection on 11–12 May 1999

Nozomu Nishitani,[1] Vladimir O. Papitashvili,[2] Tadahiko Ogawa,[1] Natsuo Sato,[3] Hisao Yamagishi,[3] Akira Sessai Yukimatu,[3] and Frederick J. Rich[4]

Received 11 September 2002; revised 2 December 2002; accepted 3 December 2002; published 15 May 2003.

[1] Ionospheric convection over the southern polar cap on 11–12 May 1999 has been studied by using the Syowa East and South HF radar data and the DMSP ion driftmeter data, when the solar wind density was very low and geomagnetic activity was low. The overall convection pattern is consistent with the previous results by *Ohtani et al.* [2000]. However, the Syowa radars and the DMSP satellites observed very high (>1500 m/s) westward plasma flows at dusk directed from the nightside toward the dayside only in the Southern (dark) Hemisphere. The high-speed flow was observed continuously across the fields of view of both radars from 1530 UT on 11 May to 0200 UT on 12 May, when the solar wind density was close to minimum. Comparison with the DMSP particle and auroral image data shows that the westward flow regions were located in the middle of the auroral precipitation area. The strong asymmetry of the convection between the two hemispheres indicates the importance of the presence (absence) of solar illumination for the absence (presence) of the strong and localized ionospheric flows. *INDEX TERMS:* 2411 Ionosphere: Electric fields (2712); 2431 Ionosphere: Ionosphere/magnetosphere interactions (2736); 2437 Ionosphere: Ionospheric dynamics; 2463 Ionosphere: Plasma convection; *KEYWORDS:* high-latitude ionospheric convection, tenuous solar wind, Syowa SuperDARN radars, DSMP driftmeter, dipolar magnetic field lines, interhemispheric asymmetry

Citation: Nishitani, N., V. O. Papitashvili, T. Ogawa, N. Sato, H. Yamagishi, A. S. Yukimatu, and F. J. Rich, Interhemispheric asymmetry of the high-latitude ionospheric convection on 11–12 May 1999, *J. Geophys. Res.*, *108*(A5), 1184, doi:10.1029/2002JA009680, 2003.

1. Introduction

[2] There have been a number of studies of the statistical convection pattern using a wide variety of observation techniques, such as polar-orbiting satellites [e.g., *Weimer*, 1995; *Papitashvili and Rich*, 2002], incoherent scatter radars [e.g., *Senior et al.*, 1990], and HF radars [*Ruohoniemi and Greenwald*, 1996]. However, most of the past studies discussed mainly the dependence of convection on the IMF; there have been few studies of the dependence on the solar wind dynamic pressure. One reason is a belief that the influence of the dynamic pressure is not as great as that of the IMF, which is more dominant, although some studies try to include dynamic pressure effects, such as the *Weimer* [2001] electric potential model. However, it should be noted that the solar wind density rarely remains below 1 cm^{-3} for prolonged periods. Therefore because of the paucity of low solar wind density data, there have been few studies of the convection pattern under tenuous solar wind conditions.

[3] It has been reported by several papers that there is asymmetry in the electric field potential in the northern and southern hemispheres [e.g., *de la Beaujardiere et al.*, 1991; *Lu et al.*, 1994]. By using the statistical Sonderstrom radar data, *de la Beaujardiere et al.* [1991] noted that there is small difference between the summer and winter cross polar cap potential, and they interpreted this in terms of the difference in the parallel potential drop due to the different ionospheric conductivity. *Lu et al.* [1994], using the AMIE algorithm, found that during the northward IMF there is a significant difference in the electric field potential in both hemispheres. It should be noted that it is not easy to compare the potential map in both hemispheres on a snapshot basis. *Papitashvili et al.* [1994] noted the difference in the electric potential in both hemispheres, but they mentioned that the difference might be due to the application of the statistical conductivity model made from the northern hemisphere data to the southern hemisphere data.

[4] From 10 to 12 May 1999 the solar wind exhibited very unusual conditions, with the density below 1.0 cm^{-3} for more than one day [e.g., *Le et al.*, 2000]. This period provides a good opportunity for studying characteristics of the ionospheric convection under extreme conditions. In this study we analyze data obtained with the Syowa East and South HF radars in Antarctica and the DMSP satellites

[1]Solar-Terrestrial Environment Laboratory, Nagoya University, Toyokawa, Aichi, Japan.
[2]SPRL, University of Michigan, Ann Arbor, Michigan, USA.
[3]National Institute of Polar Research, Itabashi-ku, Tokyo, Japan.
[4]Air Force Research Laboratory, Space Vehicles Directorate, Hanscom Air Force Base, Massachusetts, USA.

0148-0227/03/2002JA009680

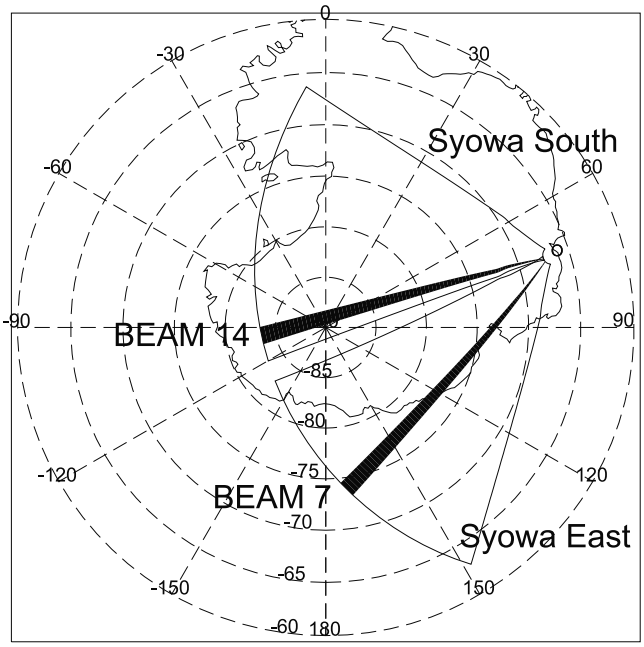

Figure 1. Distribution of the fields of view of the Syowa East and Syowa South SuperDARN radars.

to investigate the characteristics of the convection pattern and its interhemispheric asymmetry under these very unusual solar wind conditions.

2. Instrumentation

[5] The Wind satellite was in the upstream region at [35.0, −34.4, −0.2] (R_E) and at [41.7, −32.1, −9.7] (R_E) in the GSM coordinates at 0000 UT and 2400 UT, respectively, on 11 May. The spacecraft was in the solar wind for most of 11 May, but between 1730 and 1936 UT it was in the magnetosheath [*Le et al.*, 2000].

[6] The ground geomagnetic activity for this period was fairly quiet. The Kp index was 0 to 0+, and the Dst index was 0 to +10 nT on 11 May. The ground magnetograms obtained at WDC-C2 for Geomagnetism, Kyoto University (not shown) also showed the geomagnetic activity to be very low.

[7] The fields of view of the Syowa East and South radars are shown in Figure 1. The magnetic latitude and longitude are given in the Altitude Adjusted Corrected Geomagnetic Coordinate (AACGM) system, which is an updated version of the PACE geomagnetic coordinate system [*Baker and Wing*, 1989]. The magnetic local time (MLT) of Syowa Station is approximately the same as universal time (UT). During the period of interest, the radars were operated with the common program, in which each radar scanned through 16 viewing directions every 2 min. There were other SuperDARN radars operating in the Southern Hemisphere and also in the Northern Hemisphere. However, the number of ionospheric echoes received by these radars was much smaller than that for the Syowa radars. Hence in this study we only used the Syowa East/South radar data. The ion driftmeter data from the four (F11, F12, F13, and F14) DMSP satellites at an altitude of approximately 848 km are used to examine the global convection pattern and interhemispheric asymmetry. The particle, magnetic field and auroral image data from these satellites are also used to examine the precipitation characteristics.

3. Observations

[8] Figure 2 shows the magnetic field and solar wind data observed at the Wind satellite. The solar wind density was below 1.0 cm^{-3} on 11 May and as low as 0.2 cm^{-3} at about 1700 UT. It was well below 1.0 cm^{-3} between 1700 and 2400 UT. (Note that the spacecraft was in the magnetosheath between 1730 and 1936 UT [*Lazarus*, 2000].) The solar wind density was extremely low throughout the period of interest. The solar wind velocity stayed mostly between 350 and 400 km/s before 1800 UT and then, after a data gap, it dropped to below 300 km/s after 2200 UT and stayed low until 0300 UT on the next day. During the period of very low solar wind density, the IMF was mostly northward.

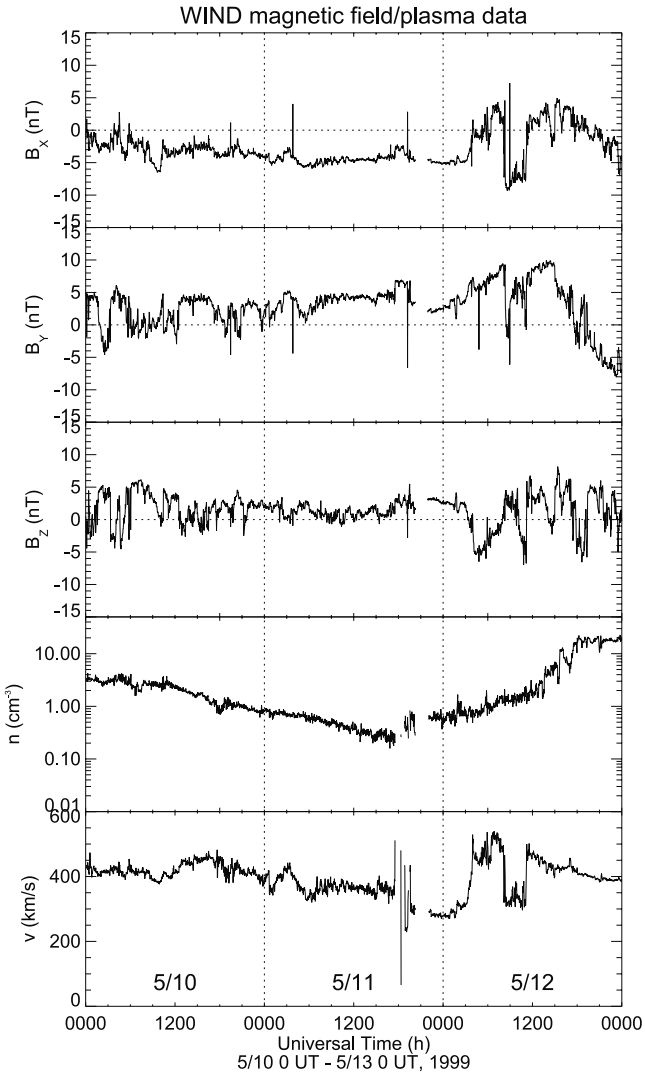

Figure 2. Variations of the Interplanetary Magnetic Field (IMF) and solar wind parameters detected by the Wind satellite from 10 to 12 May 1999.

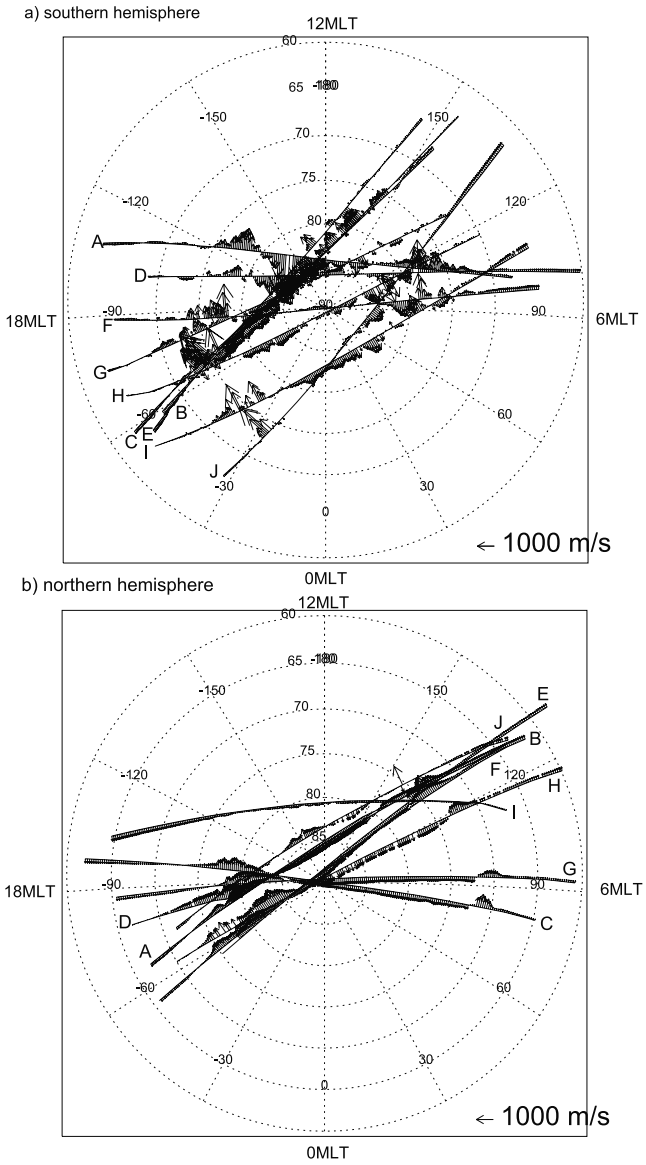

Figure 3. Summary plot of the ionospheric convection in the (a) Southern and (b) Northern Hemispheres observed by the ion driftmeters on board the DMSP satellites between 1600 UT and 2400 UT on 11 May 1999. The passes A–J are in each panel are in the chronological order.

The IMF B_y and B_x components were positive and negative respectively on 11 May.

[9] Figure 3 shows the summary plots of ion drift observed by the DMSP ion driftmeter in the Northern and Southern Hemispheres. In the figure only the data between 1600 UT and 2400 UT were plotted when simultaneous observations by the Syowa East/South radars were made in the vicinity of the satellite passes. During this period the northern polar ionosphere was solar illuminated and the southern polar hemisphere was in darkness.

[10] The overall convection pattern in the Northern Hemisphere (Figure 3b) is consistent with the results by *Ohtani et al.* [2000], who propose a large merging cell in the center of the polar cap and the distorted viscous cell in the dawn sector. As suggested by *Papitashvili et al.* [2000], the Southern Hemisphere should show the mirror image of the Northern Hemisphere convection pattern with the distorted viscous cell in the dusk because of the large positive IMF By component.

[11] On the other hand the observed intensity of the convection in the Southern Hemisphere is much stronger than that in the Northern Hemisphere. In particular we can clearly see the existence of the intense westward flow in the dusk to premidnight sector, localized to about 1 to 2 degrees in latitude in the Southern Hemisphere. The summary plot in the Northern Hemisphere shows an absence of the intense localized flow although there are much weaker but wider flows. This fact clearly indicates the asymmetry of the flow patterns between the Northern and Southern Hemispheres.

[12] The DMSP magnetic field data (not shown) indicates that the intensity of the field-aligned current in the Northern (sunlit) Hemisphere is 3 to 4 times larger than in the Southern (dark) Hemisphere. This is consistent with the interhemispheric difference in the ionospheric conductivity. The detailed relationship between the field-aligned currents and the convection will be discussed in the next section.

[13] The fast flow in the Southern Hemisphere is consistent with the Syowa SuperDARN observations, which show various temporal as well as spatial features. Figure 4 shows the range-time plots of the line-of-sight velocity on beams 7 and 14 of the Syowa East and South radars, respectively (Figure 1). The scatter region is located at high

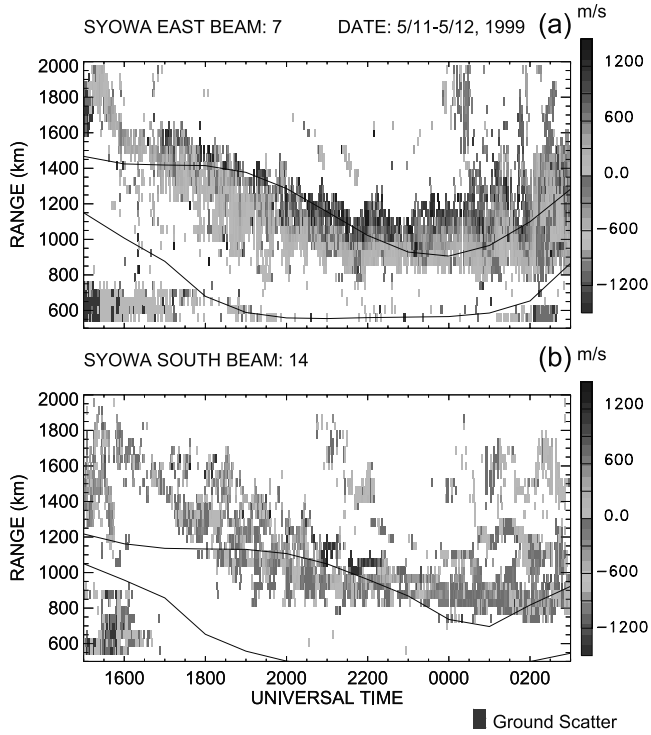

Figure 4. Range-Time-Velocity plots of the line-of-sight velocities detected by (a) beam 7 and of the Syowa East and (b) beam 14 of the Syowa South SuperDARN radars from 1500 UT on 11 May to 0300 UT on 12 May. The positive velocities are toward the radar, and negative velocities are away from the radar. The thin lines indicate the positions of the Feldstein auroral oval for very quiet conditions (Q = 0). See color version of this figure at back of this issue.

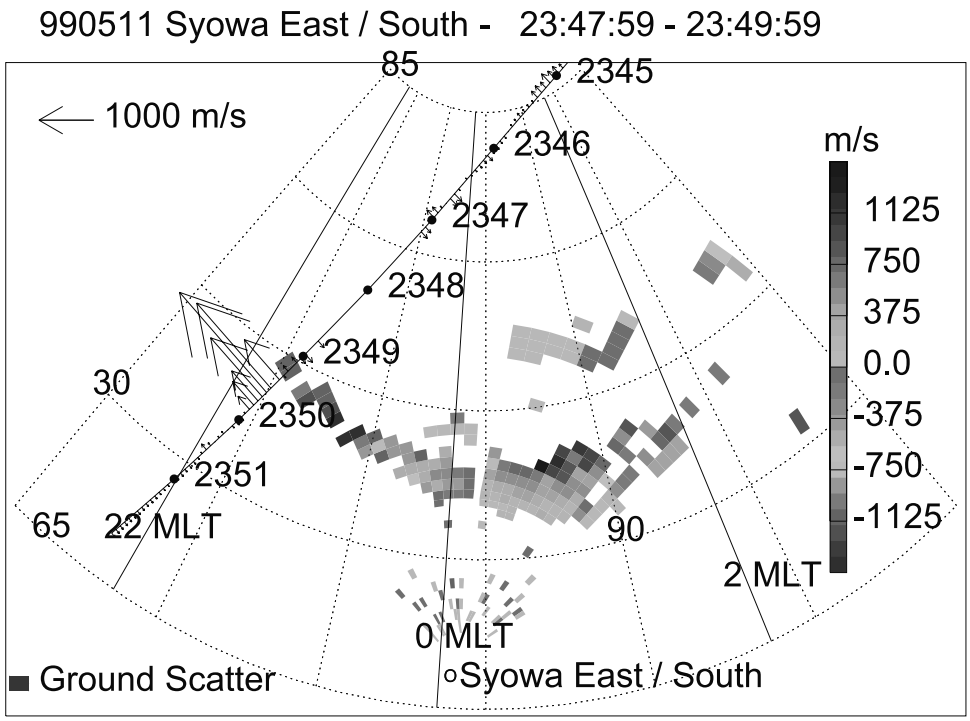

Figure 5. Two-dimensional distribution of the line-of-sight velocities obtained by the Syowa East and Syowa South SuperDARN radars from 2348 to 2350 UT. The plasma drift speed distribution measured by the ion driftmeter on board the DMSP-F12 satellite is overlaid onto the figure. See color version of this figure at back of this issue.

latitudes, near the poleward boundary of the quiet-time Feldstein auroral oval [*Holzworth and Meng*, 1975]; the poleward shift of the auroral oval region is typical for the quiet-time period but sometimes the oval moves further toward higher latitudes than the Feldstein oval under the lowest level (Q = 0) of geomagnetic activity.

[14] The echoes at the poleward edge of the scattering region show very fast flows, toward the radar at Syowa East and away from the radar at Syowa South. Figure 5 shows an example of the two-dimensional distribution of the line-of-sight velocity. It is seen that the velocity varies sinusoidally, from very strong flow toward the radar near the eastern edge of the Syowa East radar coverage to a very strong flow away from the radar near the western edge of the Syowa South radar coverage. This corresponds to the strong westward flow.

[15] We applied an L-shell fitting technique [*Ruohoniemi et al.*, 1989] to the SuperDARN data; this technique is valid when the flow is uniform in longitude and stable [*Freeman et al.*, 1991]. Figure 6 shows the result of applying that technique to the Syowa East data from 2000 UT to 2400 UT, when enough echoes were available for fitting. The data were averaged over 10 min. The figure clearly shows stable presence of the intense westward flows with the velocities of the order of 1000 to 3000 m/s. In fact there are considerable fluctuations in the flow velocity. However, the typical time scale of the flow intensity variation is longer than the scanning period of the radar (= 2 min), so these fluctuations do not affect the validity of the L-shell fitting technique. Note that a smoothing technique was applied to the data to obtain the results. The actual latitudinal width of the flow (of the order of about 2°) is shorter than their latitudinal extent in this figure.

[16] The strong westward flows seen in Figure 6 were detected simultaneously by the DMSP ion driftmeter and by the Syowa SuperDARN radars. Figure 5 shows the distribution of plasma drift velocities normal to the satellite track as detected by the DMSP-12 satellite. The data were

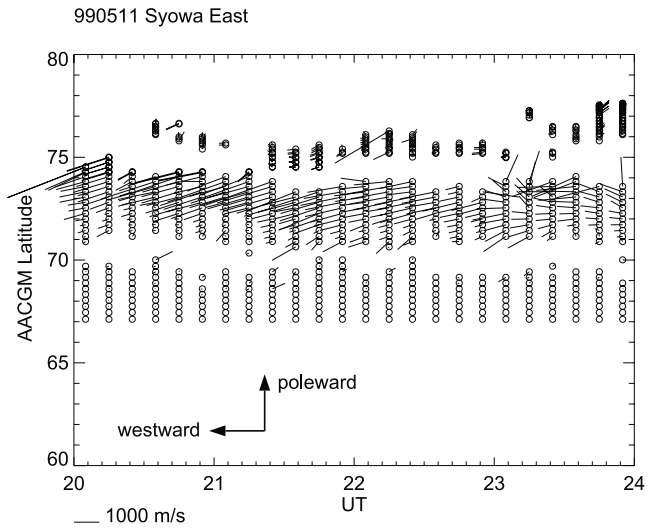

Figure 6. Distribution of the flow vectors obtained from the Syowa East radar from 2000 UT to 2400 UT on 11 May using the L-shell fitting method by *Ruohoniemi et al.* [1989].

averaged over 4 s. It is obvious that the strong flow regions identified by two different observation sources are collocated with one another. In addition the peak flow speeds (~2000 m/s) were consistent with each other. As shown in Figure 3a, we have a total of nine passes with near-simultaneous observations of the strong westward flow by the DMSP satellites and the SuperDARN radars between 1600 and 2400 UT on 11 May. All of these indicate the presence of the strong westward flow in the same latitudinal range. Furthermore, the peak plasma velocities detected by the satellite and the radar are consistent with each other.

[17] It is interesting to know which part of the particle precipitation pattern corresponds to these strong westward flow regions. In fact, there were eight passes of DMSP satellites with particle data, crossing the field of view of the Syowa East and South radars. The DMSP particle data shown in Figure 7, acquired on the pass shown in Figure 5, indicate that the high speed flow region corresponds to the higher latitude portion of the "cps" (nominally, central plasma sheet) region or to the vicinity of the boundary between the "bps" (nominally, boundary plasma sheet) and the "cps" regions, as identified by the algorithm by *Newell et al.* [1991]. In fact for all observations during that event the strong westward flow region was located in the high latitude portion of the "cps" region or around the boundary between the "bps" and "cps" regions. This fact indicates that the flow regions are located well within the open-closed boundary. The comparison with the DMSP auroral image data available for nine passes also shows that the flows were located equatorward of the auroral arcs.

[18] The DMSP magnetic field data (not shown) also shows that the flows were located near the poleward edge of the Region 2 downward field-aligned current system. For example the F12 satellite pass (marked as J in Figure 3a and in Figure 5) produces a magnetogram caused by the crossing of the broad upward R1 (near -75° latitude at 2349 UT) and then downward R2 (near -70° latitude at 2350 UT) currents as well as by another pair of opposite field-aligned currents of smaller (less than half) intensities in between. Then later currents are collocated with the strong westward flow in the ionosphere seen around -73° along the J pass in Figure 3a (and in Figure 5).

[19] The relative location of the strong flow to the auroral precipitation is consistent with the previous observation of the flow equatorward of the arc [e.g., *de la Beaujardiere et al.*, 1981] although the past observations were made mainly during geomagnetically active periods. (Please note that the relative location of the high-speed flow and auroral arc depends on the magnetic local time, and *de la Beaujardiere et al.* [1981] said that the flow equatorward of the arc is typical for the dusk to midnight sector.) The present event is different from subauroral ion drift events, which occur mainly equatorward of the diffuse auroral precipitation region under very active geomagnetic conditions.

4. Discussion

[20] We have shown the intense ionospheric flow during the period of very tenuous solar wind in the unlit southern polar cap. The overall pattern of ionospheric convection in both hemispheres is consistent with the previous result by *Ohtani et al.* [2000], who proposed a merging cell in the center of the polar cap and the viscous cell in the dawn sector in the Northern Hemisphere. *Papitashvili et al.* [2000] found supporting evidences for existence of these cells in the Northern Hemisphere from the ground geomagnetic data but failed to collect enough data from Antarctica. Nevertheless, they suggested the overall mirror image of the Northern Hemisphere convection pattern in the Southern Hemisphere, skewing the central merging cell toward dawn and putting the distorted viscous cell in the dusk sector.

[21] On the other hand, our observations with Syowa HF radars also suggest a strong asymmetry in the convection pattern between the two hemispheres. In particular, we observed very fast (>1500 m/s) westward flows in the dusk to midnight sector in the auroral oval only in the Southern Hemisphere.

[22] *Knipp et al.* [2000] calculated the overall potential pattern during the present period of interest by using the AMIE algorithm, but the pattern in the Southern Hemisphere did not show any localized intense flows in the dusk to midnight sector. One possibility is that in their algorithm the small-scale structures might have been smeared out in the global convection pattern. (In fact, the original DMSP data in their Figure 2 shows the presence of intense and localized westward flow in the Southern Hemisphere although they did not mention this in the text.)

[23] One might wonder what the generation mechanism of this fast flow is. In fact we have no firm conclusion at present. The empirical model based on the statistical observation of the DMSP satellites [*Papitashvili and Rich*, 2002] does not indicate the presence of intense and localized flows. In addition it is not easy to conceive the emergence of intense and localized flows only in the Southern Hemisphere (e.g., Figure 3) in terms of the external driving mechanisms.

[24] The original structure of the electric field should form in the magnetosphere because the structure is stable for several hours. This is also consistent with the observational result by *Le et al.* [2000] of the upward/downward field-aligned current system with latitudinally localized structure. (See their Figure 4. Note that their coordinate system is different from the AACGM coordinates used in this paper, leading to latitudinal difference of about 7 degrees.)

[25] *Golovchanskaya et al.* [2002] studied statistical characteristics of the electric field fluctuations observed by the DE 2 satellite. They found that electric field fluctuations were observed preferably during northward IMF and quiet Dst/AE activity rather than during southward IMF or high geomagnetic activity. They explained their results in terms of the interchange instability which can grow in any curvilinear magnetic field including dipolar, especially in the presence of the background field-aligned current. If we apply their theory to the present case, it is highly plausible that the localized/spiky electric field grows under the dipolar magnetic field configuration, as confirmed by the geosynchronous satellite observations [*Ohtani et al.*, 2000]. *Golovchanskaya et al.* [2002] also associated electric field fluctuations with

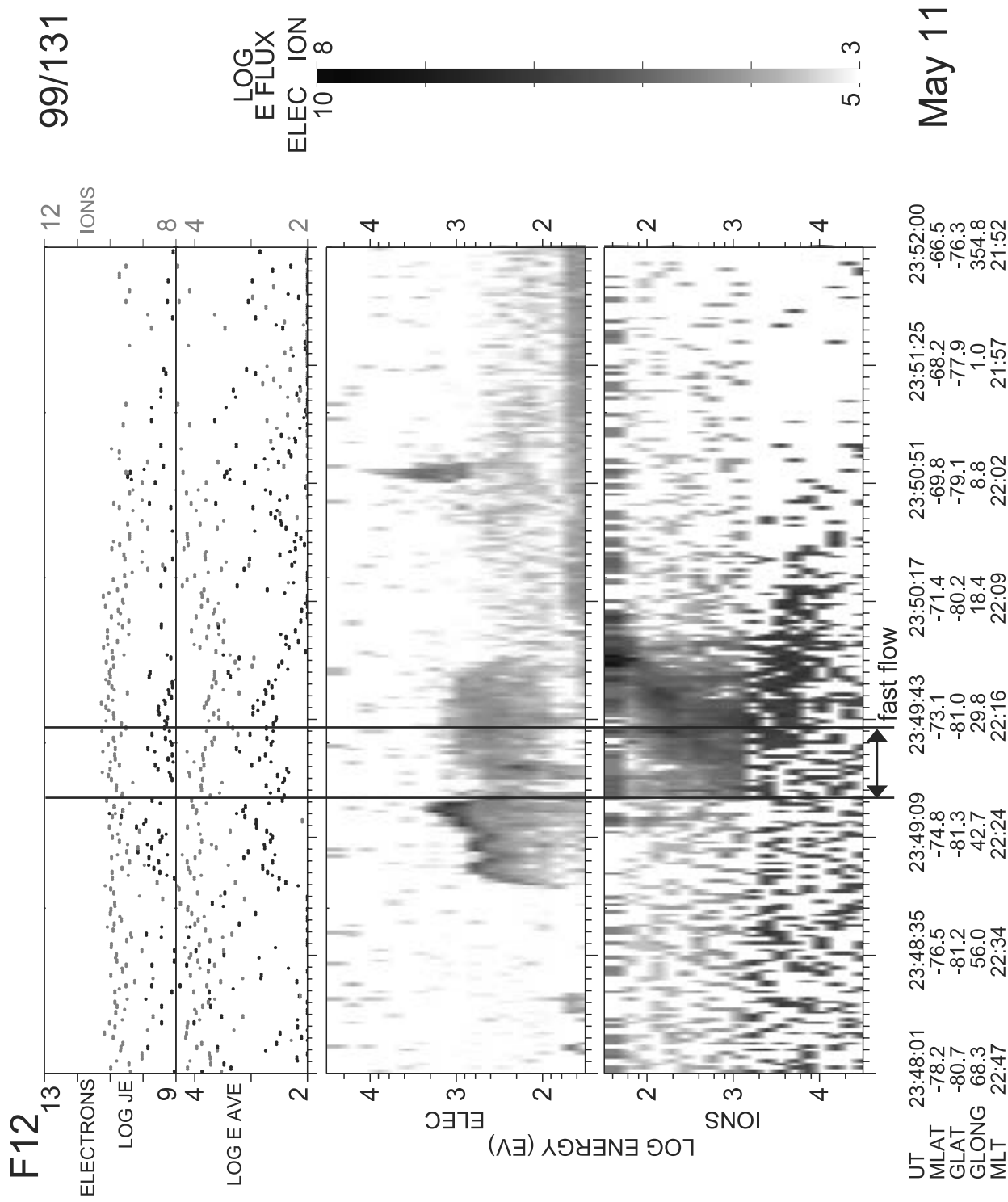

Figure 7. DMSP-F12 ion and electron spectrograms during 2348–2352 UT. The fast flow region is indicated by the arrow.

the auroral arcs, in terms of the growth of the interchange instability which requires radial density gradients as well as magnetic field curvature. This is consistent with our present event, which has close relationship with the auroral arc and auroral electron precipitation.

[26] Then the next question is whether the high-speed flow was observed only during the tenuous solar wind event. In fact, high-speed flows were observed in the previous studies. For example, *Walker et al.* [2002] has reported bursts of the westward plasma flow in the nighttime sector during intervals of constantly northward IMF. The characteristics of their flow bursts, however, are different from the present event; Walker et al.'s flow bursts are localized in space and transient, whereas our observations indicate flows which are spatially uniform in longitude and stable. Another important point is that the magnetic field was constantly highly dipolar during the period of our interest [*Le et al.*, 2000; *Ohtani et al.*, 2000], whereas *Walker et al.* [2002] reported that flow bursts occurred in association with dipolarization events. We suggest that the constantly dipolar magnetospheric configuration is suitable for sustaining intense electric field. (Note that the results by *Golovchanskaya et al.* [2002] have little information on temporal sequence because of the limitation of satellite observations.)

[27] *Le et al.* [2000] compared magnetic field configuration on 11 May 1999 observed by the Polar satellite with that on 14 May 1999, when the IMF was also weakly northward on average and the solar wind characteristics were similar except that the solar wind density was much larger. They found that the magnetic field configuration on 11 May was much more dipolar than on 14 May. We believe that this magnetic field geometry plays a crucial role in sustaining intense flows in the dusk to midnight sector. On 14 May the geomagnetic activity was also quiet and the intensity of the field-aligned currents was comparable to that on 11 May, but the SuperDARN observation shows no fast flows (data not shown).

[28] We are not certain whether the tenuous solar wind is crucial for generating intense ionospheric flow in the dark hemisphere or only prolonged northward IMF is necessary. It should be important to study a number of events with different IMF and solar wind conditions and examine the relationship between the characteristics of ionospheric flows and the external conditions. This is a subject of future studies.

[29] One might wonder what caused the strong interhemispheric asymmetry. We think that a strong candidate is the difference in ionospheric conductivities. These observations were made on 11 to 12 May when the northern polar ionosphere was solar illuminated whereas the southern polar hemisphere was in the darkness.

[30] *Weimer et al.* [1985] compared electric field changes observed by the DE-1 and DE-2 satellites, being magnetically conjugate to each other. They found that the electric field variations with shorter wavelengths ($<\sim$100 km) are more readily suppressed at the altitude of DE-2 (200 to 1000 km) than that of DE-1 ($\sim$10000 km). They interpreted this in terms of the presence of Pedersen conductivity. This interpretation can be applied to the present case; in the dark hemisphere, where the conductivity is low, the electric field in the magnetosphere is directly transferred to the ionosphere. On the other hand, in the Sun-illuminated hemisphere the conductivity is enhanced so that the localized ($<\sim$100 km) electric field structure is suppressed at the altitude of SuperDARN/DMSP observations. As a result, it is likely that the electric field structure can be seen in the dark hemisphere, but it might be smeared out in the sunlit hemisphere. Similar conclusions are also made by *Papitashvili et al.* [2002] from the study of geomagnetic substorms. They discovered that near-midnight substorms propagate to higher latitudes more often in the dark (winter) hemisphere where the ionospheric conductivity is low rather than in the sunlit (summer) polar cap.

[31] Some papers propose that the interhemispheric difference in ionospheric conductivity will lead to the difference parallel potential drop, where the larger potential drop corresponds to the smaller cross polar cap potential drop [e.g., *Volkov and Maltsev*, 1986; *de la Beaujardiere et al.*, 1991]. *Ohtani et al.* [2000] and our results show that the Northern (summer) Hemisphere has 3 to 4 times larger field-aligned currents that the Southern (winter) Hemisphere. If the larger field-aligned currents are associated with larger parallel potential drops, then it will lead to the weaker convection, which seems consistent with the present result. However, the closer look of Figure 3 indicates that the flows in the Northern Hemisphere are more extended in latitude, leading to the total potential drop comparable to the Southern Hemisphere. This cannot be explained in terms of the presence of the parallel potential drop in the sunlit hemisphere.

[32] *Volkov and Maltsev* [1986] showed in their calculation that the presence of longitudinal resistivity only in one hemisphere produces oppositely directed intense flows in both sides of the field-aligned current sheet. Our observation looks similar to the results of their calculation, although our observation shows only westward flow.

[33] Another question is why strong asymmetry exists only during this period when the solar wind was extremely tenuous. One important issue is the very weak background conductivity due to very low activity level. Under this environment the enhancement of conductivity by solar illumination is expected to play a crucial role in creating interhemispheric asymmetry in the ionospheric convection pattern.

[34] The intense westward flow region continued until 0200 UT (0300 MLT) on 12 May. It is difficult to conceive of such a distorted dusk convection cell. The statistical convection pattern [e.g., *Ruohoniemi and Greenwald*, 1996; *Papitashvili and Rich*, 2002] does not show such a distorted pattern for the same IMF orientation as in the present event. At present we do not know whether such an elongated convection cell is typical to the low-density solar wind conditions or such a latitudinally limited structure is smeared out in the statistical pattern.

[35] The total potential drop across the fast flow region, which can be calculated from the DMSP ion driftmeter data, is of the order of 10 kV. This value is consistent with the typical cross polar cap potential of 20 kV during northward IMF, although much smaller than the typical value of 100 kV during active periods. Nevertheless, owing to its localized character, this potential drop produces very high-speed flow. It will lead to strong frictional heating in the ionosphere, possibly related to several ionospheric

processes such as electron density suppression and ion upflow events [e.g., *Ogawa et al.*, 2001].

5. Conclusions

[36] During this very tenuous solar wind event we observed continuous westward flow with the speed >1500 m/s in the dusk to midnight sector in the Southern Hemisphere. This flow existed throughout the period of northward B_z. The flow region was located in the vicinity of bps/cps boundary of the auroral precipitation region. The interhemispheric asymmetry of the flow pattern strongly suggests that the difference in the solar illumination in two hemispheres plays an important role in generating intense and localized flow only in the Southern Hemisphere. This result is important for the future studies of the magnetosphere-ionosphere coupling under very unusual solar wind conditions.

[37] **Acknowledgments.** This research is supported by the Grant-in-aid for Scientific Research (A:11304029) from Japan Society for the Promotion of Science (JSPS). The Ministry of Education, Culture, Sports, Science, and Technology supports the Syowa HF radar systems. The 40th JARE carried out the HF radar operation at Syowa. VOP acknowledges support from the JSPS Senior Fellowship Program and the NSF award ATM-0112720. We also acknowledge K.W. Oglivie (NASA/GSFC) and J.T. Steinberg and A.J. Lazarus (MIT) for the use of the WIND SWE data and R. Lepping for providing the WIND MFI data. The DMSP particle data were provided by P.T. Newell at JHU/APL. The DMSP image data were provided by H. Miyaoka at NIPR. The geomagnetic indices data were provided by WDC for Geomagnetism, Kyoto University. We thank G. Rostoker and M. Lester for useful discussions.

[38] Arthur Richmond thanks I. Golovchanskaya and another reviewer for their assistance in evaluating this paper.

References

Baker, K. B., and S. Wing, A new magnetic coordinate system for conjugate studies at high latitudes, *J. Geophys. Res.*, *94*, 9139–9144, 1989.

de la Beaujardiere, O., R. Vondrak, R. Heelis, W. Hanson, and R. Hoffman, Aurora arc electrodynamic parameters measured by AE-C and the Chatanika radar, *J. Geophys. Res.*, *86*, 4671–4685, 1981.

de la Beaujardiere, O., D. Alcayde, J. Fontanari, and C. Leger, Seasonal dependence of high-latitude electric fields, *J. Geophys. Res.*, *96*, 5723–5735, 1991.

Freeman, M. P., J. M. Ruohoniemi, and R. A. Greenwald, The determination of time-stationary to-dimensional convection patterns with single-station radars, *J. Geophys. Res.*, *96*, 15,735–15,749, 1991.

Golovchanskaya, I. V., Y. P. Maltsev, and A. A. Ostapenko, High-latitude irregularities of the magnetospheric electric field and their relation to solar wind and geomagnetic conditions, *J. Geophys. Res.*, *107*(A1), 1001, doi:10.1029/2001JA900097, 2002.

Holzworth, R. H., and C.-I. Meng, Mathematical representation of the auroral oval, *Geophys. Res. Lett.*, *2*, 377–380, 1975.

Knipp, D. J., C.-H. Lin, B. A. Emery, J. M. Ruohoniemi, F. J. Rich, and D. S. Evans, Hemispheric asymmetries in ionospheric electrodynamics during the solar wind void of 11 May 1999, *Geophys. Res. Lett.*, *27*, 4013–4016, 2000.

Lazarus, A. J., The day the solar wind almost disappeared, *Science*, *287*, 2172–2173, 2000.

Le, G., C. T. Russell, and S. M. Petrinec, The magnetosphere on May 11, 1999, the day the solar wind almost disappeared: I. Current systems, *Geophys. Res. Lett.*, *27*, 1827–1830, 2000.

Lu, G., et al., Interhemispheric asymmetry of the high-latitude ionospheric convection pattern, *J. Geophys. Res.*, *99*, 6491–6510, 1994.

Newell, P. T., W. J. Burke, E. R. Sánchez, C.-I. Meng, M. E. Greenspan, and C. R. Clauer, The low-latitude boundary layer and the boundary plasma sheet at low altitude: Prenoon precipitation regions and convection reversal boundaries, *J. Geophys. Res.*, *96*, 21,013–21,023, 1991.

Ogawa, T., S. C. Buchert, N. Nishitani, N. Sato, and M. Lester, Plasma density suppression process around the cusp revealed by simultaneous CUTLASS and EISCAT Svalbard radar observations, *J. Geophys. Res.*, *106*, 5551–5564, 2001.

Ohtani, S., P. T. Newell, and K. Takahashi, Dawn-dusk profile of field-aligned currents on May 11, 1999: A familiar pattern driven by an unusual cause, *Geophys. Res. Lett.*, *27*, 3777–3780, 2000.

Papitashvili, V. O., and F. J. Rich, High-latitude ionospheric convection models derived from DMSP ion drift observations and parameterized by the IMF strength and direction, *J. Geophys. Res.*, *107*(A8), 1198, doi:10.1029/2001JA000264, 2002.

Papitashvili, V. O., B. A. Belov, D. S. Faermark, Y. I. Feldstein, S. A. Golyshev, L. I. Gromova, and A. E. Levitin, Electric potential patterns in the northern and southern polar regions parameterized by the interplanetary magnetic field, *J. Geophys. Res.*, *99*, 13,251–13,262, 1994.

Papitashvili, V. O., C. R. Clauer, F. Christiansen, V. A. Pilipenko, V. A. Popov, O. Rasmussen, V. P. Suchdeo, and J. F. Watermann, Geomagnetic disturbances at high latitudes during very low solar wind density event, *Geophys. Res. Lett.*, *27*, 3785–3788, 2000.

Papitashvili, V. O., C. R. Clauer, F. Christiansen, Y. Kamide, V. G. Petrov, O. Rasmussen, and J. F. Watermann, Near-conjugate magnetic substorms at very high latitudes observed by Greenland and Antarctic ground magnetometers and Ørsted satellite, in *Sixth International Conference on Substorms*, edited by R. M. Winglee, pp. 110–114, Univ. of Washington, Seattle, 2002.

Ruohoniemi, J. M., and R. A. Greenwald, Statistical patterns of high-latitude convection obtained from Goose Bay HF radar observations, *J. Geophys. Res.*, *101*, 21,743–21,763, 1996.

Ruohoniemi, J. M., R. A. Greenwald, K. B. Baker, J. P. Villain, C. Hanuise, and J. Kelly, Mapping high-latitude plasma convection with coherent HF radars, *J. Geophys. Res.*, *94*, 13,463–13,477, 1989.

Senior, C., D. Fontaine, G. Caudal, D. Alcayde, and J. Fontanari, Convection electric fields and electrostatic potential over $61° < \lambda < 72°$ invariant latitude observed with the European incoherent scatter facility. 2. Statistical results, *Ann. Geophys.*, *8*, 257–272, 1990.

Volkov, M. A., and Y. P. Maltsev, Longitudinal resistance in the magnetosphere-ionosphere circuit with asymmetric hemispheres, *Geomagn. Aeron.*, *26*, 875–877, 1986.

Walker, A. D. M., K. B. Baker, M. Pinnock, J. R. Dudeney, and J. P. S. Rash, Radar observations of magnetospheric activity during extremely quiet solar wind conditions, *J. Geophys. Res.*, *107*(A4), 1038, doi:10.1029/2001JA000063, 2002.

Weimer, D. R., Models of high-latitude electric potentials derived with a least error fit of spherical harmonic coefficients, *J. Geophys. Res.*, *100*, 19,595–19,607, 1995.

Weimer, D. R., An improved model of ionospheric electric potentials including substorm perturbations and application to the Geospace Environment Modeling November 24, 1996, event, *J. Geophys. Res.*, *106*, 407–416, 2001.

Weimer, D. R., C. K. Goertz, D. A. Gurnett, N. C. Maynard, and J. L. Burch, Auroral zone electric fields from DE 1 and 2 at magnetic conjunctions, *J. Geophys. Res.*, *90*, 7479–7494, 1985.

N. Nishitani and T. Ogawa, Solar-Terrestrial Environment Laboratory, Nagoya University, Toyokawa, Aichi 442-8507, Japan. (nisitani@stelab.nagoya-u.ac.jp)

V. O. Papitashvili, SPRL, University of Michigan, 2455 Hayward Street, Ann Arbor, MI 48109, USA.

F. J. Rich, Air Force Research Laboratory, Space Vehicles Directorate, 29 Randolph Road, Hanscom AFB, MA 01731-3010, USA.

N. Sato, H. Yamagishi, and A. S. Yukimatu, National Institute of Polar Research, Itabashi-ku, Tokyo 173-8515, Japan.

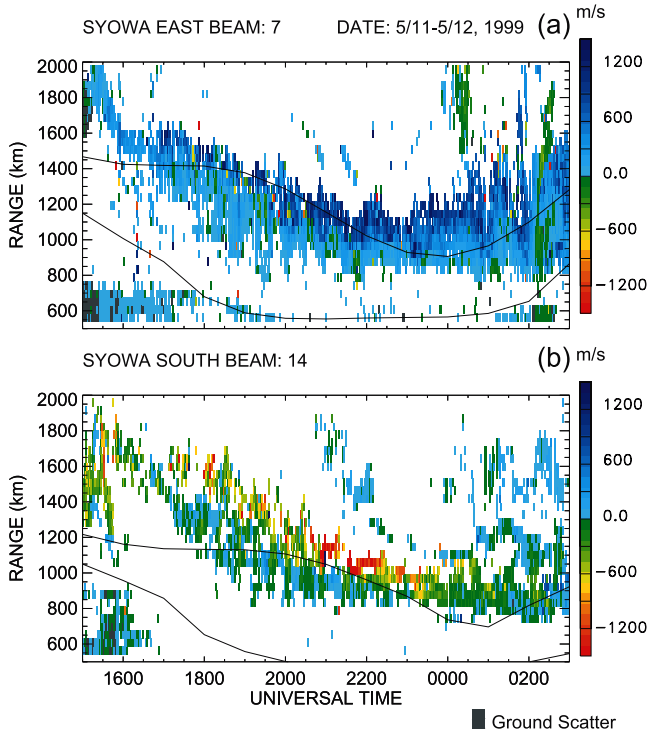

Figure 4. Range-Time-Velocity plots of the line-of-sight velocities detected by (a) beam 7 and of the Syowa East and (b) beam 14 of the Syowa South SuperDARN radars from 1500 UT on 11 May to 0300 UT on 12 May. The positive velocities are toward the radar, and negative velocities are away from the radar. The thin lines indicate the positions of the Feldstein auroral oval for very quiet conditions (Q = 0).

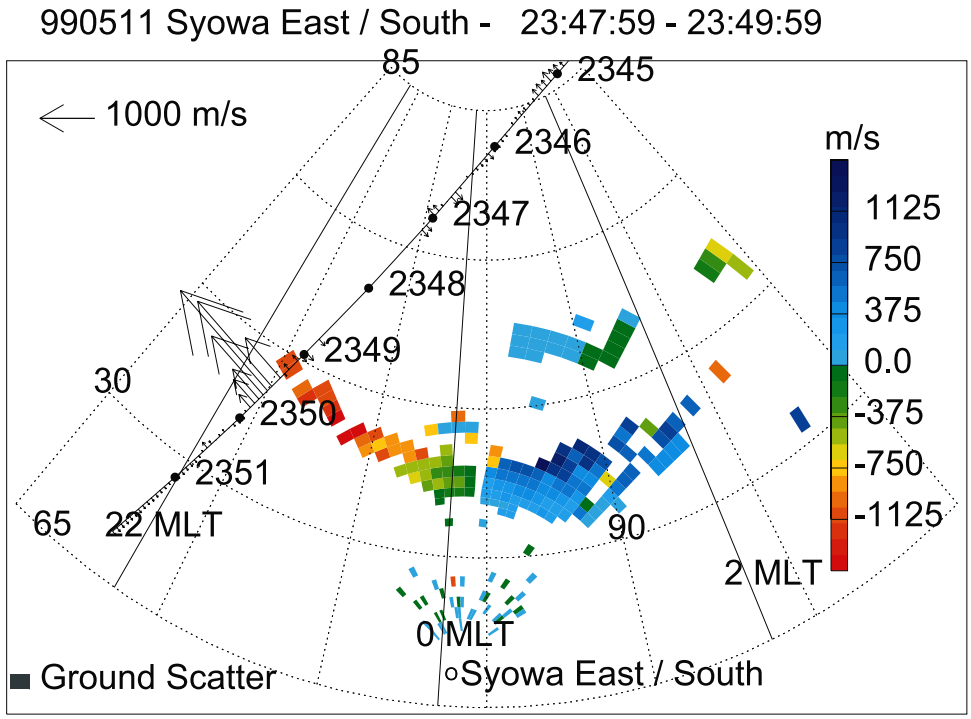

Figure 5. Two-dimensional distribution of the line-of-sight velocities obtained by the Syowa East and Syowa South SuperDARN radars from 2348 to 2350 UT. The plasma drift speed distribution measured by the ion driftmeter on board the DMSP-F12 satellite is overlaid onto the figure.